

Prediction of a Shape-Induced Enhancement in the Hole Relaxation in Nanocrystals

Marco Califano,* Gabriel Bester, and Alex Zunger

National Renewable Energy Laboratory, Golden, Colorado 80401

Received May 21, 2003; Revised Manuscript Received July 30, 2003

ABSTRACT

We present a pseudopotential calculation of the single particle and excitonic spectrum of CdSe nanocrystals. We find that in the excitonic manifold derived from the ground state electron and the first 60 hole states there are two energy gaps much larger than the typical LO phonon energy in bulk CdSe. Such gaps can effectively slow the hole relaxation process, as recently found experimentally. We show that they originate from two gaps in the hole spectrum and are therefore a *single-particle* effect, as opposed to an *excitonic* effect. The calculated width of the gaps increases with decreasing dot size, in agreement with the experimental trend of the energy loss rate that decreases with dot size. We find that the presence of the gaps is not limited to CdSe nanocrystals with the wurtzite crystal structure but is also found in spherical InAs zinc blende dots. Comparison with our results for quantum rods and cylinders of different aspect ratios, and with a single-band effective mass model, shows the origin of the gaps to be interband coupling in spherical NCs. The gaps disappear above an aspect ratio of about 3–4, thus predicting a fast hole relaxation for elongated nanostructures.

The single-particle energy levels in CdSe nanocrystals (NCs) exhibit typical spacings between electron states of the order of hundreds of meV, and typical energy separations between hole states of the order of 1–10 meV. This structure, peculiar to 0D systems, was thought^{1,2} to lead to a “phonon bottleneck” in the electron relaxation from an excited level to the ground state, since the energy of a LO phonon in bulk CdSe (~26 meV) is much smaller than the interelectronic level spacing (300 meV for a 1.9 nm CdSe NC). It was therefore expected that the lifetime of an excited electron would be rather long. Surprisingly, experiments measure a very fast decay for an excited p electron,^{3–5} with typical lifetimes that decrease with size from 530 to 120 fs for dots with $R = 4.1$ to 1.7 nm, i.e., much faster than those relative to phonon-assisted relaxation. This fast decay has been explained^{3–5} in terms of an Auger-like relaxation⁶ (Figure 1, step I), whereby the excited electron can relax to its ground state and the excess energy is transferred via Coulomb scattering to the hole (which, depending on the experimental setup, might also be excited in our “initial state”), that is promoted deep into the valence band. Provided that the spacing between hole levels be of the order of phonon energies, the hole can then relax very quickly to the top of the valence band by emitting phonons (Figure 1, step II).

Recently, however, Xu et al.⁷ found a dramatic reduction in the hole energy-loss rate (HELRL) in the final stage of the hole relaxation in CdSe NCs: they observed an initial fast

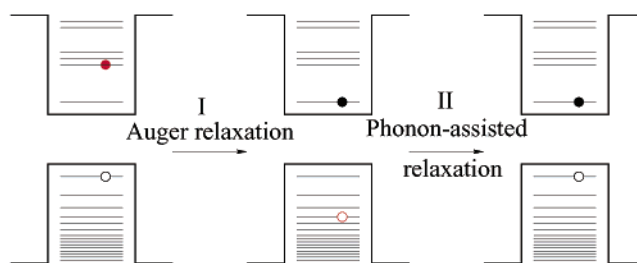


Figure 1. Schematics of the electron Auger thermalization (step I) and subsequent hole relaxation (step II).

relaxation with a nearly constant rate over a wide energy range, followed by a slow relaxation, the spectral onset of which was size dependent. In contrast to electron relaxation that becomes faster with decreasing dot size (strongly suggesting a nonphonon mechanism, e.g., Auger-like thermalization), HELRLs *decrease* with decreasing dot size, indicating a different process from Auger. This was found⁷ to be independent of the NC surface passivation (both TOPO-capped CdSe NCs and TOPO-capped CdSe/ZnS core/shell dots were considered) and type of solvent used (hexane and toluene), which ruled out the possibility of invoking a coupling to surface defects to explain slow hole thermalization. Coupling to phonons was therefore proposed as the underlying mechanism for hole relaxation, also due to the fact that the observed initial fast relaxation rates were close to those estimated for hole-LO phonon interactions in bulk CdSe. The reduction of the HELRL in the final stage of the

* Corresponding author.

hole relaxation was then attributed by the authors to the opening of a gap in the excitonic manifold between an “absorbing” state $E_{\pm 1}^U$ and an “emitting” state $E_{\pm 1}^L$.⁸ Analysis⁹ shows that $E_{\pm 1}^U$ is a $\{h_2, e_1\}$ (i.e., electron ground state and second hole state) derived exciton, whereas $E_{\pm 1}^L$ is a $\{h_1, e_1\}$ (i.e., electron and hole ground state) derived exciton. Hence, according to Xu and co-workers,⁷ the gap is due to many-body (exchange-related) fine structure associated with (h_2, e_1) vs (h_1, e_1) .

In this work we will use our semiempirical pseudopotential method to show that (i) there are actually two gaps in the excitonic spectrum of CdSe NCs; these gaps are indeed much larger than the typical LO phonon energy in bulk CdSe and therefore both can effectively slow the hole relaxation process; (ii) consequently, the HELR is predicted to change twice (as opposed to once); this is found to be in agreement with the experimental data; (iii) the larger gap increases with decreasing NC size in agreement with the experimental findings of a HELR that decreases with decreasing dot size; (iv) *the gaps originate from deep states (h_4, h_5 , not h_1, h_2), in the hole spectrum and are a single-particle effect, as opposed to an excitonic (i.e. many-body) effect*, as proposed by Xu and co-workers; (v) their presence is not limited to CdSe NCs with the wurtzite crystal structure but is also predicted in spherical InAs zinc blende dots; their origin is in the spherical shape of the NC. Elongated rod-like NCs are predicted to have no such gaps once the axial ratio exceeds 3–4, and therefore are expected to exhibit fast hole relaxation.

Theoretical methods that were previously applied to nanocrystals¹⁰ provided information only on the first few valence eigenvalues and did not detect any gap in them. Furthermore, the $\mathbf{k}\cdot\mathbf{p}$ approach, when applied to small dots, has been shown¹¹ to miss many energy eigenvalues near the top of the valence band on account of its overestimate of the hole confinement. Nor are gaps found in simple models, like the one-band effective mass or particle-in-a-sphere (with infinite barrier potential). Figure 2a, shows the energies of the first 10 states below the top of the valence band, corresponding to an energy range of ~ 0.7 eV, for $R = 20$ Å, calculated within the particle-in-a-sphere model. The typical interlevel spacings obtained in this approach for a hole effective mass value of $1.3m_0$ (CdSe¹²) are of the order of 40–80 meV, for $R = 20$ Å, and no proper “gaps” (i.e., spacings much larger than the typical spacing) are found in the valence band. There is therefore a need for a more accurate theoretical treatment to explain the origins of these gaps.

Here the single-particle energy levels ϵ_i were computed with the empirical pseudopotential method described in ref 13, solved within a plane-wave basis, including spin-orbit effects. The surface of the wurtzite dots is saturated by ligand potentials.¹⁴ We use the potential of ref 9. We consider three dots: Cd₈₃Se₈₁, Cd₂₃₂Se₂₃₅, and Cd₅₃₄Se₅₂₇ of diameters 20.66, 29.25, and 38.46 Å, respectively. We also performed calculations on three rods, with the same short axis $R_s = 29.25$ Å and aspect ratios Q of long axis over short axis R_l/R_s of about 2, 3, and 4, and on three CdSe cylinders with

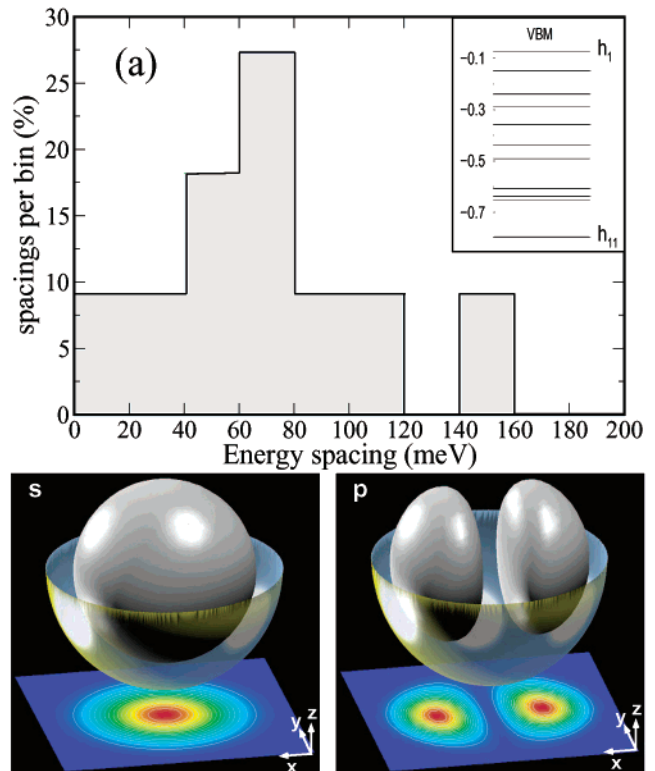


Figure 2. Results for the “particle in a sphere” model, with infinite potential barrier. (a) Mainframe: energy spacing between consecutive hole levels in a spherical CdSe NC with $R = 20$ Å. The sampling bin is 20 meV. Inset: hole spectrum for the same QD. (b) Wave functions squared for the (pure) s and p states. The yellow shell represents (half) the dot surface. The plane on the bottom of each panel shows a section through the dot center.

the same diameter ($d = 29.25$ Å) and aspect ratios of height over diameter of 2, 3, and 4. The geometry of the rods is ellipsoidal with the long axis oriented along the z (c) wurtzite axis. With the single-particle orbitals we construct a set of 840 single-substitution Slater determinants. The exciton wave functions are then expanded in this basis set,⁹ and the many-particle Hamiltonian is solved via CI.

For CdSe spherical dots we computed the first 60 bound hole states below the top of the valence band, corresponding to an energy range of ~ 0.5 eV for the largest dot and of ~ 1 eV for the smallest (see inset in Figure 3a). We found that the hole spectra of all dots considered exhibit similar characteristics. As shown in the histogram in Figure 3a for Cd₅₃₄Se₅₂₇, the typical interlevel spacings are of the order of 1–10 meV, (slightly larger, 1–20 meV, for the smallest dot, due to increased confinement), with only a few energy levels separated by more than 25 meV. We label the ground hole state (HOMO) as h_1 ($E_{h_1} \equiv E_v$) and the excited states as h_n , with n increasing with decreasing hole energy. The LUMO is e_1 . The hole single-particle manifolds for all dots present two gaps that are larger than the typical LO phonon energy in bulk CdSe: the largest gap g_1 (of the order of $4\hbar\omega_{LO}$ or more) is always found between the levels h_4 and h_5 (i.e., at $E_v - 40$ meV for the largest dot and at $E_v - 95$ meV for the smallest dot); the second gap g_2 (of about $2\hbar\omega_{LO}$) is deeper in the valence band and may have different positions in

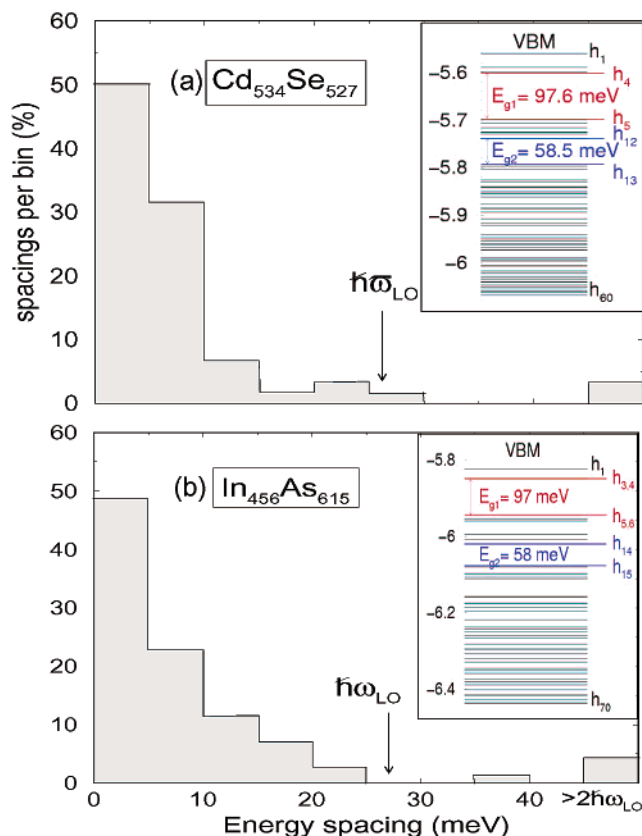


Figure 3. Pseudopotential calculation. Energy spacing between consecutive hole levels in NCs with $R = 19 \text{ \AA}$: (a) $\text{Cd}_{534}\text{Se}_{527}$, (b) $\text{In}_{456}\text{As}_{615}$. The sampling bin is 5 meV. Insets: hole spectrum for the same QD.

different dots (it is located between levels h_{12} and h_{13} , i.e., at $E_v - 180 \text{ meV}$, in $\text{Cd}_{534}\text{Se}_{527}$; between h_{13} and h_{14} , i.e., at $E_v - 270 \text{ meV}$, in $\text{Cd}_{232}\text{Se}_{235}$; and between levels h_{15} and h_{16} , i.e., at $E_v - 420 \text{ meV}$, in $\text{Cd}_{83}\text{Se}_{81}$).¹⁵ Both gaps can effectively slow the hole relaxation process. It is important to notice that the gaps originate from h_4 and h_5 and deeper states and not from h_1 and h_2 , as implied by Xu and co-workers.⁷

Possible explanations of the origin of the gaps within the valence band could be: (i) the wurtzite structure and the resulting crystal field splitting; (ii) some special features specific to the CdSe material; (iii) an effect of the dot passivation, or, finally, (iv) the shape of the NC. To investigate these aspects further, we performed additional calculations for a spherical InAs zinc blende, colloidal dot ($\text{In}_{456}\text{As}_{615}$), with the same dimensions ($R = 19 \text{ \AA}$) as the $\text{Cd}_{534}\text{Se}_{527}$ dot. For this dot the single-particle problem was solved by expanding the dot wave functions as a linear combination of bulk Bloch states (LCBB).¹⁶ The dot was passivated by embedding it in a lattice matched higher band-gap material as it is done in core/shell structures. As shown in Figure 3b, the hole manifold for the InAs NC is similar to that obtained for the CdSe dot (Figure 3a). The average interlevel spacing is almost the same as that calculated for the CdSe NC, and we find the same two gaps appearing in its hole spectrum. Both gaps have the same width (to within less than 1%) as the ones we found in the CdSe NC, with

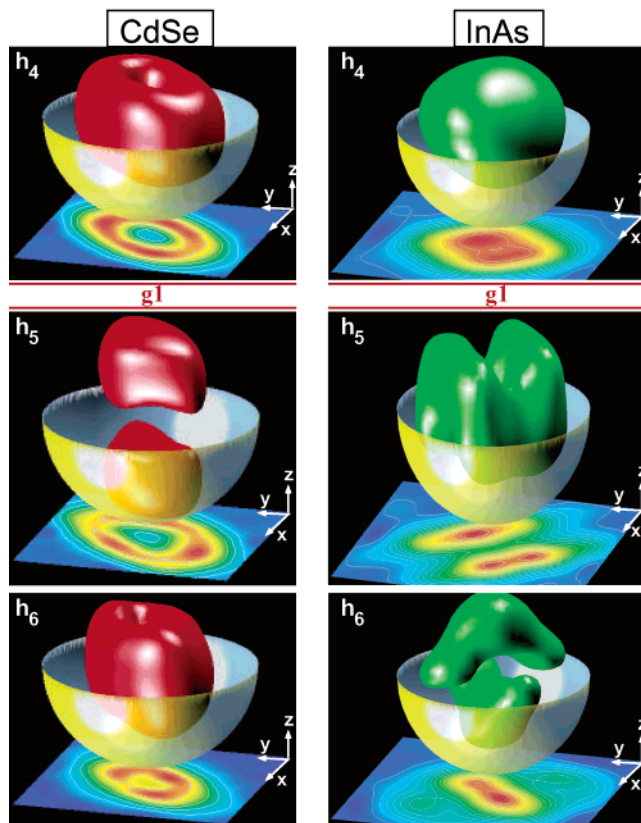


Figure 4. Envelope functions squared for hole states above and below the largest gap $g1$ in NCs with $R = 19 \text{ \AA}$: CdSe, left-hand side, InAs, right-hand side. The yellow shell represents (half) the dot surface. The plane on the bottom of each panel shows a section through the dot center.

the largest gap again found between the levels $h_{3,4}$ and $h_{5,6}$ (in this case doubly degenerate due to the T_d symmetry of the system) at $E_v - 25 \text{ meV}$, and the second gap found between the levels h_{14} and h_{15} , at $E_v - 200 \text{ meV}$. Figure 4 shows the envelope functions of the states below and above the largest gap $g1$ for both CdSe (left-hand side) and InAs (right-hand side) NCs with $R = 19 \text{ \AA}$. For InAs we find, on both sides of this gap, states with prevalent p character: on the high energy side, they also have considerable s (and little d and f) component, whereas on the low energy side they have considerable d and f (and little s) component. Note that in the single-band approximation (Figure 2), the levels have pure symmetries (i.e., either s, or p, or d, etc.), and no gaps within the valence band. *The existence of the gaps therefore reflects inter-band mixing effects in spherical NCs.*

The question now arises as to whether the shape of the NC is relevant for the presence of the gaps in the hole manifold. We therefore performed calculations on CdSe ($R_s = 29.2 \text{ \AA}$) and InAs ($R_s = 38 \text{ \AA}$) ellipsoidal quantum rods (QRs) with different aspect ratios Q_{QR} ranging from 1 (spherical dot) to 4. Figure 5 shows the energy of the first 9 hole states at the top of the valence band (out of the 20 calculated), as a function of the aspect ratio Q_{QR} , for CdSe QRs with $R_s = 29.2 \text{ \AA}$. We find that already for $Q_{QR} = 2$ the gap $g1$ is reduced to almost one-third (51 meV) of the value it assumes for $Q_{QR} = 1$ (129 meV). On the other hand, for $Q_{QR} = 2$ another gap (probably derived from $g2$) opens

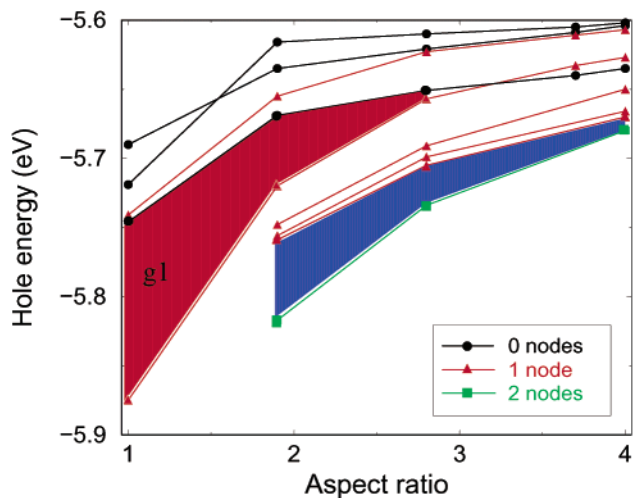


Figure 5. Energy of the first 9 hole states below the top of the valence band, as a function of the NC aspect ratio, for CdSe QRs with $R_s = 29.2 \text{ \AA}$. The different hole states are labeled according to the number of nodes of the wave function along the z direction (long rod axis R_l). The shaded areas indicate the evolution with Q of the two gaps larger than $\hbar\omega_{\text{LO}}$.

between the states h_8 and h_9 (58 meV). For $Q_{\text{QR}} \sim 3$ there are three gaps of the order of about 30 meV between the states h_3-h_4 (29 meV), h_5-h_6 (34 meV), and h_8-h_9 (29 meV). Gaps of this size should, however, not compromise the efficiency of the hole relaxation.^{17,18} All these gaps decrease to a value below the LO phonon energy for $Q_{\text{QR}} = 4$, for both CdSe and InAs rods. A previous pseudopotential calculation¹⁹ of electronic states versus aspect ratio for CdSe quantum rods of similar sizes as those considered in this work investigated the behavior as a function of Q_{QR} (starting from $Q_{\text{QR}} = 1$) of only the first 4 hole states below the top of the valence band and therefore did not include the evolution of the gaps we are interested in.

To further investigate the shape dependence of the valence band gaps, we performed calculations on quantum cylinders (QCs) with the same dimensions as the rods (i.e., $h = R_l$ and $d = R_s$), and therefore the same aspect ratios $Q_{\text{QC}} = Q_{\text{QR}}$. We found that already for $Q_{\text{QC}} = 2$ there are no gaps larger than $\hbar\omega_{\text{LO}}$ in the hole manifold. The gaps therefore originate from the spherical shape of the dots, and their width decreases with elongation. Note that the occurrence of the gaps is indeed a *shape* effect, as opposed to a *volume* effect (i.e., the gap decreases with increasing NC elongation, but not because of the volume increase). In fact, if the important quantity were the volume, the CdSe rod with $R_s = 29.2 \text{ \AA}$ and aspect ratio $Q_{\text{QR}} = 2$, having a smaller volume than the CdSe spherical NC with radius $R = 19.2 \text{ \AA}$ should have a larger gap. As seen in Figure 5, its gap g_1 is instead half as large as that of the spherical dot.

The presence of valence band gaps in spherical NCs is also expected to affect the impact ionization rates (IIRs) in these systems. In an impact ionization process, a hot electron in level e_n decays to the LUMO (e_1) and excites a valence electron across the band gap. For a given electronic excess energy $\Delta_x = E_{e_n} - E_{e_1}$, impact ionization will not occur if $(E_{e_1} - E_{h_4}) < \Delta_x < (E_{e_1} - E_{h_5})$, or, in other words, if the

energy made available in the $e_n \rightarrow e_1$ decay process is larger than the energy needed to promote a valence electron from h_4 (above the valence gap) to e_1 , but smaller than that required to excite an electron from h_5 (below the valence gap) to e_1 . This energy interval has the width of the valence gap g_1 ($\sim 100-180 \text{ meV}$) and depends on the dot size. When this condition is satisfied there are no valence electrons available to be promoted to the LUMO, while satisfying energy conservation. Note that since $E_{e_2} - E_{e_1} > 3E_{g_1}$, and $E_{h_1} - E_{h_4} < E_{g_1}/2$, Δ_x is not enough to excite an electron from h_1 to e_2 . The impact ionization efficiency, therefore, drops in that energy interval. This is not the case in the bulk, where the IIR is an increasing function of Δ_x .

The presence of valence band gaps might have important consequences on Auger *electron* relaxation processes (Figure 1, step I) as well. In a typical experimental setup,²⁰ a visible pump pulse creates an excited electron-hole pair, and a time-delayed infrared pulse is used to reexcite the electron within the conduction band. If (i) the hole is generated in a state deeper than h_5 , and (ii) the electron reexcitation within the conduction band as well as (iii) the Auger electron relaxation are both faster than the phonon-assisted hole relaxation across the gap g_1 , then the electron might relax from e_2 to e_1 by exciting the hole from h_5 rather than from h_1 . In some experimental configurations,⁵ however, the hole is always allowed to relax to the ground state before the electron is reexcited from e_1 to e_2 by a IR post-pump.

We next examine whether many-body effects (accounted for through CI) alter the gaps seen in the single-particle spectrum (Figure 3). In our CI calculations we include (i) electron-hole Coulomb attraction, responsible for the creation of bound excitons, (ii) electron-hole exchange interaction, which splits excitons into spin manifolds. For example,⁹ the $\{e_1, h_1\}$ ground-state exciton is 4-fold (spin) degenerate in the single-particle approach. The electron-hole exchange interaction splits it into two doublets: the lowest in energy is spin forbidden (dark), whereas the highest in energy is spin allowed (bright). We calculated the excitonic (CI) spectrum for all three CdSe NCs, including 30 hole and 7 electron states. We find that the same two gaps that were found in the single-particle hole spectrum now appear in each exciton manifold. The origin of the gaps is therefore a single-particle effect. The width of the gap decreases with increasing e_n (the electron level from which the exciton manifold is derived). Figure 6 shows the excitonic spectrum for Cd₅₃₄Se₅₂₇: we see that the first two gaps (g_1 and g_2) are derived from the electron ground state (and from the same hole states, $\{h_4, h_5\}$, and $\{h_{12}, h_{13}\}$ as in the single-particle case), whereas progressively higher gaps (g_3, g_4 , etc.), are derived from increasingly higher electron states (and the same hole states).

In Figure 7 we present a comparison between the energy gaps calculated in the single-particle (empty circles and solid lines) and CI (solid squares and dashed lines) approach, plotted as a function of NC radius. Only the first three gaps (see Figure 6) are shown. We find that: (i) E_{g_1} increases with decreasing dot radius, consistently with the experimental finding⁷ that the HELR decreases (i.e., the lifetime increases)

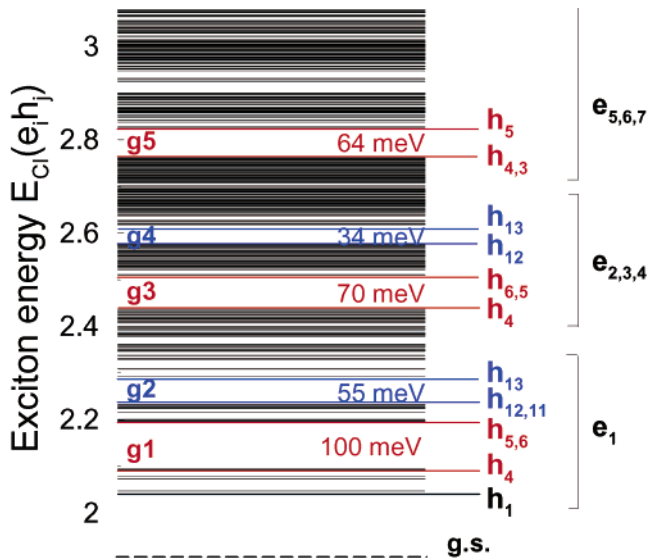


Figure 6. CI excitonic spectrum for $\text{Cd}_{534}\text{Se}_{527}$. We denote the single-particle origin of the excitons in terms of the levels with high contributions to the CI states.

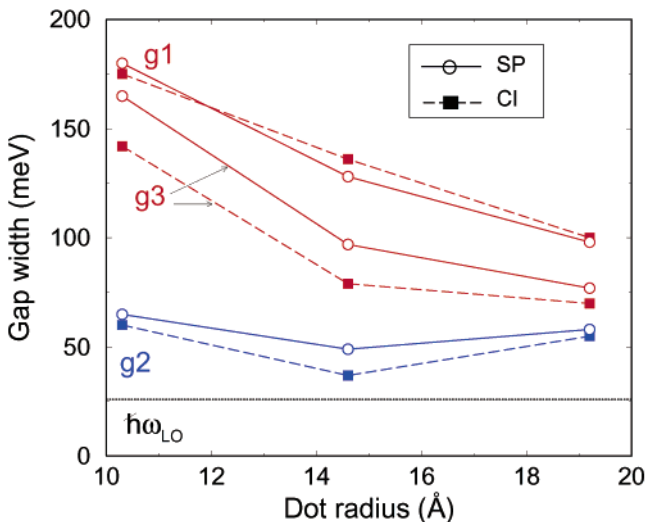


Figure 7. CdSe: excitonic energy gaps calculated in the single-particle (SP, empty circles and solid lines) and CI (solid squares and dashed lines) approach, plotted as a function of NC radius.

with decreasing dot size; (ii) conversely, E_{g2} is rather independent of R ; (iii) both E_{g1} and E_{g2} are almost unaffected by many-body effects (the single-particle results almost coincide with the CI ones, excepted for the $R = 14 \text{ \AA}$ dot); (iv) many-body effects reduce higher gaps (the ones derived from excited electron states) compared to their single-particle values, with larger effects the smaller the dot (see curve relative to $g3$ in Figure 7). Therefore the *existence* of the gaps is a single-particle effect whereas their *width* is influenced by many-body effects.

Finally we compare our predictions with experiment. Figure 8 shows the measured energy-loss curve⁷ for a 1.8 nm CdSe NC (solid circles and lines). Xu and co-workers⁷ have identified two slopes in that curve, with the change of slope occurring close to the energy of about 2.22 eV, corresponding to the measured position of the 1S absorption

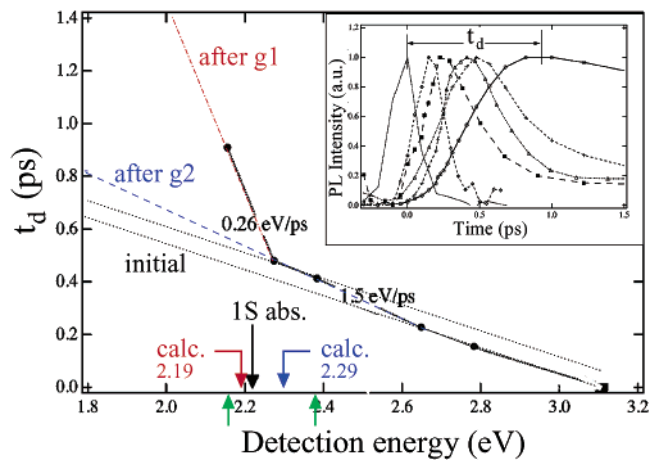


Figure 8. Changes in slope of the hole energy-loss curve (i.e., the time delay t_d of the “hot” PL maximum with respect to a pump pulse [see inset], plotted as a function of the detection energy): experimental data for a 1.8 nm dot (solid circles, solid line, and HELR values) and theoretical predictions for a 1.9 nm dot (the red and blue arrows mark the upper energy end of the gaps). The dotted, dashed and dash-dotted lines emphasize the different slopes in the experimental energy-loss curve (HELRL = dE/dt_d). The green arrows indicate the positions of the first experimental points that determine a new slope in the curve. The black arrow indicates the position of the measured 1S absorption, around which position Xu and co-workers⁷ identify the only change in slope in the HELRL they consider.

resonance, indicated by a vertical black arrow. This implies the existence of a single gap within the valence band, located around $\sim E_v - 70 \text{ meV}$ for that specific dot size. Analysis of their data, however, reveals three different slopes in the energy-loss curve, indicated by the extrapolated lines in Figure 8. These slopes correspond to the initial HELRL (dotted line), the HELRL after $g2$ (dashed line), and the HELRL after $g1$ (dash-dotted line). Since the experimental configuration consists of a hot hole h_n and a ground-state electron e_1 , no gap other than $g1$ and $g2$ is relevant in Figure 8 (higher gaps involve different electron states). We see that our identification of two gaps (Figures 3 and 6) is consistent with the appearance of three slopes in the measured energy-loss curve. Furthermore, the calculated positions of the change in slope (2.29 and 2.19 eV, indicated by blue and red arrows in Figure 8) are in good agreement with the experimental curve,²¹ considering that the calculations were performed for a slightly larger dot than the experimental one, which yields energy values shifted slightly to the red, compared to those relative to the experimental dot. The presence of a gap ($g2$) between two sets of closely spaced energy levels, could, however, also generate a step-like jump in the delay time, where the hole relaxation would be fast above the gap, slow across the gap, and then fast again below the gap, with the slope being approximately the same above and below the step. The parallel dotted lines in Figure 8 show that this scenario is also supported by the experimental data: due to the large energy interval between two consecutive experimental points, such jump in the delay time could have occurred anywhere between the two measurements at 2.38 and 2.65 eV and have been therefore undetected. The (dotted) line through the points at 2.27 and 2.38 eV is consistent with a parallel to

the (dotted) line passing through the experimental points for higher energies. It has to be mentioned, however, that the first change of slope (the first reduction of the HELR) might also be within the experimental error, whereas the second is definitely not. In other words, the slopes of the dotted and dashed lines in Figure 8 might be the same within experimental error, whereas the dash-dotted line has an indisputably different slope. That is probably the reason Xu et al. in their work⁷ only referred to the latter change of slope (black arrow). It has to be pointed out, however, that whereas Xu and co-workers⁷ situate the drop in the HELR at energies just *below* the first absorption peak 1S (located at 2.2 eV, black arrow in Figure 8), according to our calculations (see Figure 6), both gaps are found at energies *above* the 1S absorption (which is due to exciton levels originating from h_1 , h_2 and e_1). Judging from the experimental curve alone, though, it cannot be excluded that the decrease in the HELR occur just above 2.2 eV, the last experimental point before the change of slope being at 2.27 eV and the next at 2.16 eV.

Based on the similarities found between the hole manifolds in CdSe and InAs NCs, and the fact that the LO phonon energies in both bulk materials are also very similar ($\hbar\omega_{LO}^{CdSe} \sim 26$ meV, $\hbar\omega_{LO}^{InAs} \sim 27$ meV), we predict the same pattern for the hole thermalization in InAs NCs, i.e., an as yet unobserved three-step hole relaxation.

In summary, we have used our pseudopotential calculations to explain the experimental findings of a reduction in the HELR in the final stages of the hole relaxation in CdSe quantum dots, in terms of the presence of two gaps in the excitonic spectrum. They have been shown to derive from two gaps in the hole spectrum which appear unmodified in the exciton manifold derived from the ground-state electron and the first 60 hole states. By comparison with the results obtained for quantum rods and cylinders with the small axis equal to the NC diameter and different aspect ratios, the origin of these gaps has been shown to be the spherical shape of the NCs, as opposed to the crystal wurtzite structure of CdSe. Furthermore it is shown that the existence of the gaps reflects interband mixing effects, as they are absent in a

single-band, particle in a sphere, description. An as yet unobserved three-step hole relaxation in InAs NCs is also predicted.

Acknowledgment. This work was supported by the U.S. DOE, OER-BES, Division of Materials Science.

References

- (1) Bockelmann, U.; Bastard, G. *Phys. Rev. B* **1990**, *42*, 8947.
- (2) Benisty, H.; Sotomayor-Torres, C. M.; Weisbuch, C. *Phys. Rev. B* **1991**, *44*, 10945.
- (3) Klimov, Victor I.; McBranch, Duncan W. *Phys. Rev. Lett.* **1998**, *80*, 4028.
- (4) Klimov, V. I.; Mikhailovsky, A.; McBranch, D. W.; Leatherdale, C. A.; Bawendi, M. G. *Phys. Rev. B* **1999**, *61*, R13349.
- (5) Guyot-Sionnest, Philippe; Shim, Moonsub; Matranga, Chris; Hines, Margaret *Phys. Rev. B* **1999**, *60*, R2181.
- (6) Efros, Al. L.; Kharchenko, V. A.; Rosen, M. *Solid State Commun.* **1995**, *93*, 281.
- (7) Xu, S.; Mikhailovsky, A. A.; Hollingsworth, J. A.; Klimov, V. I. *Phys. Rev. B* **2002**, *65*, 045319.
- (8) Efros, A. L.; Rosen, M. *Phys. Rev. B* **1996**, *54*, 4843.
- (9) Franceschetti, A.; Fu, H.; Wang L.-W.; Zunger, A. *Phys. Rev. B* **1999**, *60*, 1819.
- (10) Ekimov, A. I.; Hache, F.; Schanne-Klein, M. C.; Richard, D.; Flytzanis, C.; Kudryavtsev, I. A.; Yazeva, T. V.; Rodina, A. V.; Efros, Al. L. *J. Opt. Soc. Am. B* **1993**, *10*, 100.
- (11) Fu, H.; Wang, L.-W.; Zunger, A. *Phys. Rev. B* **1998**, *57*, 9971.
- (12) Hermann, C.; Yu, P. Y. *Phys. Rev. B* **1980**, *21*, 3675.
- (13) Wang, L.-W.; Zunger, A. *Phys. Rev. B* **1995**, *51*, 17 398. Fu, H.; Zunger, A. *Phys. Rev. B* **1997**, *56*, 1496.
- (14) Wang, L.-W.; Zunger, A. *Phys. Rev. B* **1996**, *53*, 9579.
- (15) In addition to these two gaps, which are common to all three dots considered, there are additional gaps, none of them larger than $2\hbar\omega_{LO}$, located in different positions for different dots: in Cd₈₃Se₈₁ between h_1 and h_2 (43 meV) and between h_2 and h_3 (40 meV); in Cd₂₃₂Se₂₃₅ between levels h_{15} and h_{16} (40 meV).
- (16) Wang, L.-W.; Zunger, A. *Phys. Rev. B* **1999**, *59*, 15806.
- (17) Li, X. Q.; Nakayama, H.; Arakawa, Y. *Phys. Rev. B* **1999**, *59*, 5069.
- (18) Inoshita, T.; Sakaki, H. *Phys. Rev. B* **1992**, *46*, 7260.
- (19) Hu, J.; Wang, L.-W.; Li, L.-S.; Yang, W.; Alivisatos, A. P. *J. Phys. Chem. B* **2002**, *106*, 2447.
- (20) Klimov, Victor I. *J. Phys. Chem. B* **2000**, *104*, 6112.
- (21) We'd like to emphasize that the energy-loss curve changes slope for the first time (corresponding to the first slowing down of the hole relaxation), around the energy of 2.38 eV (green arrow in Figure 8). The change of slope, in fact, is determined by the position of the first experimental point *outside* the dotted line connecting the points at high detection energies, and not by the position of the last experimental point *on* that line.

NL0343304